

General Disclaimer

One or more of the Following Statements may affect this Document

- This document has been reproduced from the best copy furnished by the organizational source. It is being released in the interest of making available as much information as possible.
- This document may contain data, which exceeds the sheet parameters. It was furnished in this condition by the organizational source and is the best copy available.
- This document may contain tone-on-tone or color graphs, charts and/or pictures, which have been reproduced in black and white.
- This document is paginated as submitted by the original source.
- Portions of this document are not fully legible due to the historical nature of some of the material. However, it is the best reproduction available from the original submission.

DOE/NASA/2674-79/4
NASA TM-79140

(NASA-TM-79140) MHD PERFORMANCE
CALCULATIONS WITH OXYGEN ENRICHMENT (NASA)
32 p HC A03/MF A01 CSCL 10A

N79-25499

Unclassified
G3/44 23393

MHD PERFORMANCE CALCULATIONS WITH OXYGEN ENRICHMENT

C. C. P. Pian, P. J. Staiger,
and G. R. Seikel
National Aeronautics and Space Administration
Lewis Research Center

Work performed for
U.S. DEPARTMENT OF ENERGY
Office of Energy Technology
Division of Magnetohydrodynamics

Prepared for
Eighteenth Symposium on
Engineering Aspects of Magnetohydrodynamics
Butte, Montana, June 18-20, 1979



NOTICE

This report was prepared to document work sponsored by the United States Government. Neither the United States nor its agent, the United States Department of Energy, nor any Federal employees, nor any of their contractors, subcontractors or their employees, makes any warranty, express or implied, or assumes any legal liability or responsibility for the accuracy, completeness, or usefulness of any information, apparatus, product or process disclosed, or represents that its use would not infringe privately owned rights.

DOE/NASA/2674-79/4
NASA TM-79140

MHD PERFORMANCE CALCULATIONS
WITH OXYGEN ENRICHMENT

C. C. Pian, P. J. Staiger,
and G. R. Seikel
National Aeronautics and Space Administration
Lewis Research Center
Cleveland, Ohio 44135

Prepared for
U. S. DEPARTMENT OF ENERGY
Office of Energy Technology
Division of Magnetohydrodynamics
Washington, D. C. 20545
Under Interagency Agreement EF-77-A-01-2674

Eighteenth Symposium on
Engineering Aspects of Magnetohydrodynamics
Butte, Montana, June 18-20, 1979

MHD PERFORMANCE CALCULATIONS WITH OXYGEN ENRICHMENT

C. C. P. Pian, P. J. Staiger, and G. R. Seikel
NASA Lewis Research Center
Cleveland, Ohio 44135

SUMMARY

The effect of oxygen enrichment of the MHD combustion air on the channel and plant performance has been studied for the ECAS-2 type plants. The MHD channel power output is optimized as a function of various generator parameters and physical constraints. The salient differences between the maximum power and maximum net power generators are described. Directly and indirectly-preheated plant performances with O_2 enrichment are calculated. Results show that there is an optimum level of oxygen enrichment for each given plant type, preheat temperature, and assumed oxygen production cost. The optimum degree of enrichment rises with decreasing preheat temperature. Using current O_2 production costs, oxygen enrichment was found to be beneficial for directly-preheated plants if the preheat temperature is less than 1800 to 2200F. Oxygen enrichment was found to be advantageous in separately-fired plants for preheat temperatures less than 2500 to 3000F. However, this performance gained due to enrichment in the separately-fired plants must be weighted against the increased capital cost of having both a separately-fired preheater system and an oxygen plant.

This report emphasizes the performance aspects of MHD plants using oxygen enrichment. Results of ongoing air-separation plant studies (managed by NASA and funded by DOE) will be required to define the cost of electricity.

INTRODUCTION

Numerous studies have considered oxygen enriching the combustion air to increase the performance of open-cycle MHD power plants and/or to reduce their development time and developmental cost¹. It is rather difficult to compare the results of these studies due to the differing cost and technological assumptions. However, they generally concluded that oxygen enrichment can increase the enthalpy extraction from the MHD generator at a given oxidant preheat temperature. In addition, oxygen enrichment at moderate preheat temperatures permits replacement of the expensive and complex regenerative air heater systems with more conventional metal-alloy heat exchangers. The calculated cost of electricity and the relative performance benefits gained (or lost) from oxygen enrichment are extremely sensitive to the assumed power and costs to produce the oxygen, the channel design assumptions, and the plant design. The effects of plant design include such factors as separately-fired preheat versus direct preheat, integration of the air separation plant with the MHD/steam plant, etc.

More recently, oxygen enrichment was considered as one of the options in the Parametric Study of Potential Early Commercial (PSPEC) MHD Plants studies. These investigations were conducted to identify attractive near-term plant designs having an acceptable performance and cost of electricity but with some lower technology components than plants defined by previous studies such as ECAS.

One of the parametric cases investigated by General Electric in ECAS-1², however, considered oxygen enrichment as an alternative to directly-fired high-temperature preheat. Only one value of preheat temperature and percent oxygen enrichment was assessed. Results indicated that an O₂ enriched plant may be competitive in cost of electricity but lower in thermodynamic performance. In reference 3, preliminary considerations were given to the effects of O₂ enrichment on the ECAS-2 MHD plant performance. Results indicated that the plant efficiency can generally be improved by enrichment but this requires a substantial increase in the plant pressure ratio. Separately-fired preheater plants benefited more from oxygen enrichment than directly-preheated plants. The oxygen enrichment analysis in reference 3 was centered on studying the effect of plant configuration on the overall plant performance. For this reason some simplifying assumptions were made on the channel performance characteristics.

The effect of O₂ enrichment on the performance of ECAS-2 advanced commercial plants is re-evaluated in this report. Consideration is given to the generator design. The MHD plants herein have performance which is optimized as a function of percent oxygen enrichment, preheat temperature, and generator electrical constraints. The optimum degree of oxygen enrichment is a function of preheat temperature and whether the plant has a directly or separately-fired preheater. The effects due to the choice of oxygen plant used and the way the oxygen plant is integrated with the remainder of the MHD plant are also investigated.

CHANNEL PERFORMANCE CALCULATIONS

The overall performance of an MHD plant is strongly dependent on the MHD generator performance. It is, thus, important to use a generator design that maximizes the overall plant efficiency. In this respect, it is generally not desirable to operate the MHD generator at its maximum power-out condition, since compressor work must be considered. A method of optimizing the channel design is reviewed herein and the channel performance characteristics for various values of preheat temperature and degrees of oxygen enrichment are presented.

The generators considered in this study are for the generator thermal flow rate of the ECAS-2 plant: $5373 \text{ MW}_{\text{th}}$. The coal is Illinois #6; the seed is potassium carbonate; the oxidant is air or oxygen-enriched air. Other design parameters are listed in Table I. Boundary conditions are specified at the two ends of the MHD generator. The total enthalpy at the channel inlet is the enthalpy after the combustion less the heat loss in the combustor and nozzle. The ECAS-2 value of combustor/nozzle heat loss is assumed. The stagnation pressure at the diffuser exit is taken to be 1.14 atm. Generally, the ECAS-2 diffuser pressure recovery coefficient of 0.7 and a constant generator length of 25 meters are assumed in this study. The sensitivity of generator performance to shorter channels and less efficient diffusers is, however, presented in a later section.

It was found in past oxygen enrichment studies that better performance could be obtained if the combustor pressure and channel length were allowed to increase with increasing oxygen enrichment. This can, however, result in channels that are unrealistically long. Therefore, in this analysis the channel was kept at a constant length.

The generator calculations are performed with a quasi-one-dimensional flow model. This model consists of an inviscid central core flow with boundary layers developing along the walls. The turbulent boundary layers are treated by a momentum integral approach. The thermodynamic and transport properties of the gas are calculated following Svehla and McBride, ref. 4; the procedure given in reference 5 was used to compute the electrical properties of the gas. The electrode voltage drop distributions are assumed to be of the form:

$$V_d = a + b\delta^*$$

where δ^* is the boundary layer displacement thickness. The constants a and b are those used by Avco/G.E. in ECAS-2⁶. Although a and b generally should be functions of the generator operating conditions, they are kept constant in the present analysis to limit the complexity of the generator model. The results to be presented herein are for generators operating at an approximately constant Mach number ($\gamma_s M^2 = \text{constant}$). Comparison between the performance of the approximately constant Mach number and the constant velocity generator designs was presented earlier in reference 3 for representative ECAS-2 cases.

The method of reference 7 is used to determine the optimum streamwise variation of duct parameters for a generator with prespecified length, diffuser exit pressure, and streamwise distribution of generator velocity or Mach number. The optimization is performed subject to limits on the Faraday current density, J_y ; the Hall field, E_x ; the total electric field, $E = \sqrt{E_x^2 + E_y^2}$; and the Hall parameter, β . At every streamwise location, the magnetic induction, B , and the load factor, K , are adjusted to the maximum values that would still satisfy all of the following conditions:

$$\beta \leq \beta_{\text{crit}} \quad (1)$$

$$K \geq 1 - \frac{|J_y|_{\text{crit}}}{\sigma u B} \quad (2)$$

$$K \geq 1 - \frac{|E_x|_{\text{crit}}}{\beta u B} \quad (3)$$

$$E = \sqrt{E_x^2 + E_y^2} \leq |E|_{\text{crit}} \quad (4)$$

$$K \geq K_{\text{min}} \quad (5)$$

$$B \leq B_{\text{max}}. \quad (6)$$

The values of B_{max} , $E_x|_{\text{crit}}$, $|J_y|_{\text{crit}}$, and β_{crit} are picked to reflect the state of magnet and channel technology. The channel operating life is strongly influenced by the values assigned to these limits. For the Faraday generator, the insulating sidewalls are subjected to electrical fields in both the axial and transverse directions. In order to limit the electrical stress on the sidewalls, the total electric field strength is bounded by condition (4) in the

present optimization procedure. In selecting a suitable value for E_{crit} , one must consider such factors as: the particular sidewall design, the materials of construction, etc. Whether or not the transverse electric field, E_y , should be limited instead of E would also depend on the actual sidewall design. In that case, $E_y \leq E_{y_{crit}}$ would replace condition (4). K_{min} denotes the minimum allowable value of the load parameter and is used as a control parameter in the calculation procedure.

The optimum streamwise distributions of B and K are determined by defining a generator design which is limited at each station by two appropriate criteria. Which two criteria are dominant at a location depends on the operating conditions and the assumed values for the electrical and magnet constraints. For example, near the generator inlet, the design point is usually determined by the limitations specified in equations (2) and (4). Near the generator exit, limits (1) and (3) will most likely predominate. The optimum magnetic field profiles obtained in this manner can be used as guidelines by the magnet designers. Once the magnet design is fixed, the generator loading can be reoptimized with conditions (1) and (6) replaced by the actual magnetic field profile.

The optimization of a Faraday channel loading has been investigated previously by Doss and Geyer⁸ but with a different formulation and procedure. The criteria for controlling the load factor in their sectional optimization scheme were the electrical strength of the

channel in the longitudinal direction and the Faraday current density. The magnetic field was assumed constant at a value of 5 Tesla.

The typical variation of power out for an MHD generator is shown in figure 1. In this case MHD combustor oxidizer is 2500F preheated air. The gross MHD power as a function of the minimum load factor, K_{min} , is shown in figure 1a. The dashed lines denote lines of constant chamber pressure. The net channel power out, MHD minus compressor power, versus the MHD combustor pressure, P_c , is plotted in figure 1b. In the computation of compressor power, an initial oxidant temperature of 60F and a compressor polytropic efficiency of 0.898 are assumed. A pressure drop of 0.195 P_c is assumed between the air compressor and the MHD combustor. As indicated in figure 1a, there is a maximum power and corresponding combustor pressure which the specified length (25 meter) generator can be operated at without exceeding the specified electric and magnetic stresses. Or in effect for a given combustor pressure there is a minimum length channel. The most desirable operating combustor pressure is, however, at the maximum of the net power curve, figure 1b.

The channel design is vastly different for the maximum power and maximum net power generators. In figure 2, distributions of the electrical variables and the magnetic field for these two generator designs are compared. For this example, the maximum net power generator operates at $P_c = 9$ atm. The channel has a constant load parameter, $K = 0.798$. Conditions (4) and (5) dominated over major portions of this generator design. The maximum power generator has a

higher combustor pressure of 12.78 atm and variable loading is required. The load factor tends to decrease near the channel entrance (trend dictated by conditions (2) and (4)), then increases rapidly downstream (trend dictated by conditions (3) and (4)). The β_{crit} condition prevails beyond ≈ 23 meters thus causing the drop in the magnetic field and K profiles.

The J_y , E_x , and K distributions for the maximum power design are similar to the results obtained by Doss and Geyer (ref. 8) using their sectional optimization technique. It cannot be guaranteed, however, that the "local" approach characteristic of the present formulation and that of reference 8 will yield the global optimum generator⁹.

A typical generator performance map as a function of oxygen enrichment is presented in figure 3 for a low temperature (1100F) MHD combustor oxidizer preheat. The generator/diffuser adiabatic efficiency is defined as the MHD power divided by the change in enthalpy the flow would have in expanding from the total pressure at the generator inlet to that at the diffuser exit. In these design calculations the thermal input to the generator was kept constant at the 5373 MW_{th} level by adjusting the mass flow rate for the various values of percent oxygen enrichment. A constant seed/coal weight ratio was maintained with varying oxygen enrichment to insure adequate seed for sulfur removal. The degree of oxygen enrichment is given by:

$$\text{percent oxygen enrichment} = 100 \times \left(1 - \frac{N/O}{3.26} \right)$$

where N/O is the nitrogen/oxygen mass ratio in the oxidant.

Cross plotted in figure 3 are P_c , K_{min} , and the channel heat loss, Q . The generator heat loss was calculated by integrating the turbulent heat flux over the generator wall surface. The slag-coated walls were assumed to be at 1700K (ECAS-2 value). Both P_{MHD} and Q increase with increasing P_c and percent oxygen enrichment. Also note that for a given P_c , there is a value of oxygen enrichment which maximizes P_{MHD} . This value of enrichment increases with increasing P_c . The range of maximum net MHD power out is also indicated in figure 3.

One can still extract 15% of the flow enthalpy in the MHD generator at 1100F preheat and no oxygen enrichment. For this case, the generator mass flow and channel volume are, respectively, 1.21 and 1.6 times greater than the General Electric ECAS-2 generator.

For a given preheat temperature, a set of electrical and magnet constraints, and a specified air separation plant performance characteristic, the maximum net MHD power can be determined as a function of percent oxygen enrichment. This is accomplished by considering only the MHD generator-compressor subsystem. However, to determine the optimum value of oxygen enrichment, one must evaluate the combined performance of both the oxygen plant and the MHD plant.

PLANT PERFORMANCE

Plant performance is compared herein on the basis of plant thermodynamic efficiency. The definition of thermodynamic efficiency is as in ECAS: the gross AC power output divided by the higher heating value of the coal input to the plant. It may be written

$$\eta_T = \bar{P}_{NET} (1 - \eta_S) - \bar{P}_0 - \bar{f} + \eta_S (1 + \bar{P}_S - \bar{P}_L)$$

where

$$\bar{f} = (1 - \eta_I) \bar{P}_{MHD} - (1 - \frac{\eta_S}{\eta_C}) \bar{P}_{CPR} - (1 - \frac{\eta_S}{\eta_0}) \bar{P}_0$$

and

P_{MHD} is the MHD generator DC output.

P_{CPR} is the power required to drive the cycle compressor.

$P_{NET} = P_{MHD} - P_{CPR}$

P_0 is the power used to drive the air separation plant compressors, if required.

P_F is the power in the fuel input to the plant (to both the MHD combustor and the oxidant preheater system) based on its higher heating value.

P_S is the power in the seed associated with converting it from K_2CO_3 to K_2SO_4 .

P_L is the sum of stack losses and other losses and also includes the power required for coal drying.

η_S is the efficiency of the steam turbine-generator cycle.

η_C is the efficiency of the steam turbine cycle which drives the MHD compressor.

η_0 is the efficiency of the steam turbine cycle which drives the air separation plant compressor.

η_I is the efficiency of the DC-AC inverter.

The overbars denote quantities nondimensionalized with respect to the fuel input power P_F .

From the expression for $\bar{\eta}_T$ it is clear that for a given level of oxygen enrichment, $\bar{\eta}_T$ will be very close to its maximum if \bar{P}_{NET} (or \bar{P}_{NET}) is maximized. The small quantity \bar{f} , which includes the effects of inverter efficiency and of differences in steam cycle efficiencies, will have only a very minor influence on the point where $\bar{\eta}_T$ is maximum. Table I lists the important cycle parameters and performance assumptions used in the plant performance calculations.

The separately-fired plants analyzed used an atmospheric pressure reheat for the preheater system with an assumed energy conversion efficiency. The results presented herein are based on energy conversion efficiency of 90% of the preheater coal higher heating value. The combustion air used by the preheater combustor was recuperatively preheated to 1100F in all cases. This air was mixed with an amount of recycled stack gases, also preheated to 1100F, to give a 300F approach temperature difference between the streams at the hot end of the preheater. The approach temperature difference at the cold end of the preheater was also kept fixed at 300F.

Figure 4 shows the relative efficiencies of a number of MHD/steam plants with various types of preheater and oxidant preheat temperatures as a function of oxygen enrichment at a fixed oxygen production energy requirement. For reference, the efficiency of the ECAS-2 MHD/steam plant is also indicated.

Figure 4 confirms the general trends shown in reference 3. Oxygen enrichment offers a greater performance benefit at lower preheat temperatures and may actually decrease performance at higher preheat temperatures. Separately-fired plants benefit more from oxygen enrichment than do directly-fired plants operating at the same preheat temperature. As discussed above, the MHD combustor pressure is determined by maximizing P_{NET} . This pressure increases with increasing oxygen enrichment.

The relatively larger gain in performance (as oxygen enrichment is increased towards its optimum level) for the lower preheat temperatures is a result of the much larger gain in the channel power output as a fraction of the coal input to the plant. Considering only directly-fired plants for the moment, several effects may be identified as the level of oxygen enrichment increases. The power in the gas stream between the diffuser exit and the stack decreases relative to the power in the coal input to the plant. This power in the gas stream is used by the bottoming plant and for oxidant preheat. The power required for oxidant preheat decreases because of the decrease in oxidant mass flow rate and the increase in compressor exit temperature. The power required to drive the MHD compressor and the air separation plant compressor increases slightly, because the effect of the increased pressure ratio and increased enrichment outweighs the decrease in oxidant flow. The net result is a decrease in steam ~~turbo-generator output relative to plant coal input.~~ For the lower preheat plants, the gain in the MHD generator power output relative to

plant coal input is sufficient at lower but not at higher oxygen enrichment levels to overcome the decrease in bottoming plant output; thus, there is an optimum enrichment which maximizes the thermodynamic efficiency of the plant. For the higher preheat plants, the MHD generator output is not sufficient to overcome the decrease in bottoming plant output and air is the optimum oxidizer. Similar considerations apply to separately-fired plants.

In the case of directly and separately-fired plants at the same oxidant preheat temperature, the greater gain (or lesser penalty) in cycle performance of the separately-fired plant with increasing enrichment is primarily the result of the gain in channel output as a percentage of the total coal input to the plant. The amount of coal to the MHD combustor changes in the same way with changes in enrichment for both plants, but the fraction of the total coal going to the preheater combustor decreases with enrichment in the separately-fired plant. This is because the preheat power required decreases with oxygen enrichment (as a result of the decrease in oxidant mass flow rate and the higher pressure ratio) even though the amount of recuperation decreases (because the combustion gas outlet temperature from the preheater is higher).

The curves in figure 4 show that for each plant type and preheat temperature, there is an optimum level of oxygen enrichment. This optimum level increases with decreasing preheat temperature. In figure 5 the efficiencies at optimum enrichment have been plotted as a function of oxidant preheat temperature for both directly and

separately-fired plants and for two levels of oxygen production power requirement. Also shown is the performance with air as the oxidant. The merging of the separately-fired and directly-fired curves at 800F is a result of the assumptions regarding the preheater approach temperature differences and the amount of preheater combustion air and recycle gas preheat.

PERFORMANCE VARIATION WITH ASSUMPTIONS

Due to the nature of the generator optimization scheme used, the generator's operating constraints (i.e., B_{\max} , $E_{x_{\text{crit}}}$, and E_{crit}) are very influential on its performance. As an example, figure 6a shows the generator net power versus MHD combustor pressure for different sets of assumed physical constraints. For $E_{x_{\text{crit}}} = 2500$ V/m, $E_{\text{crit}} = 4000$ V/m, and $J_{y_{\text{crit}}} = 10,000$ A/m² (approximately the electrical stress limits in present generator endurance tests), no further increase in power-out is possible if the magnetic field strength limit is increased (except at nonoptimally high values of P_c). Only by increasing the limits on the electrical constraints can a higher magnetic field strength be utilized. As shown, however, operation at higher values of electrical stress offers significant performance improvement.

Figure 6b shows the sensitivity to combustor slag rejection. Whether the ECAS-2 assumption of 85% slag rejection can be accomplished is not known at this time. Whether one can maintain 85% slag rejection with oxygen enrichment (leading to higher flame temperatures) is even more speculative. For this reason, channel calculations for different

amounts of slag rejection were carried out to assess the effect of slag on the generator performance. Figure 6b shows the net MHD power decreases with decreasing slag rejection. This is only due to the effect of lower electrical conductivity. A detailed analysis of the fluid dynamic, heat transfer, and electrical effects of the slag layers were not included in the generator model used to evaluate these results.

Generator performance for two different channel lengths are shown in figure 6c. The two lengths, 25 and 20 meters, correspond respectively to the overall length of the ECAS-2 magnet and the length of its high-field portion. The thermodynamic efficiency of a direct-preheated plant using the 20-meter channel is 53.76 as compared to an efficiency of 54.45 for the 25 meter case. In the latter case, a smaller fraction of the power is produced by the steam bottoming cycle.

Large variation in the boundary layer blockage was observed during the parametric calculations of generator performance reported herein. The blockage is greater in the higher oxygen-enriched cases. This trend is primarily caused by our constant generator length and constant thermal input assumptions which resulted in higher values of L/D for oxygen-enriched channels. Since the diffuser performance is strongly influenced by the inlet blockage, the diffuser efficiency should decrease as a function of increasing oxygen enrichment. To appraise the effect of diffuser pressure recovery on generator performance, calculations using less efficient diffusers were carried out. Typical results are shown in figure 6d. A slightly higher operating pressure is desired for the poorer performing diffuser case. Representative results of the plant thermodynamic efficiency are given in Table II.

Figure 7 shows the variation of generator performance as a function of the initial states of the MHD combustor oxidant. Two different states of the oxidant prior to the air compressors are considered. In one case, the oxidant is assumed to be a blend of air and product gas from the air separation plant, both available at 60F and ambient pressure. In the second case, the oxidant is assumed to be a blend of air initially at 1 atm and 60F and enriched air (0.41 molar fraction oxygen) initially at 3 atm and 80F. The pressurized 0.41 molar enriched stream is from one of the possible single-column air separation plants under consideration, reference 10. One will notice that the value of optimum P_c utilizing the enriched product gas at elevated pressures are generally 1/2 to 1 atm higher than those cases using the product gas at ambient pressure.

One type of air separation plant configuration being considered can yield product gas which is moisture free. The beneficial effect of this moisture reduction in the oxidant blend on the channel performance was also assessed. For the 62.37% oxygen-enriched case, all of the moisture in the oxidant can be removed by the 0.41 molar single-column oxygen plant. At 1100F preheat, this results in a 0.35% increase in P_{MHD} over the case where the oxidant has 0.6% moisture by weight. Of course, additional improvements would be expected if greater moisture was initially present in the oxidizer.

REFERENCES

1. Petrick, M.; Shumyatsky, B. Ya.; and Koryagina, G. M.: Technical and Economic Aspects of Open-Cycle MHD Power Plants. Open-Cycle Magnetohydrodynamic Electrical Power Generation, M. Petrick, ed., Argonne National Laboratory; Moscow, Izdatel'stvo Nauka, 1978, pp. 88-126 (and references therein).
2. Comparative Evaluation of Phase I Results from the Energy Conversion Alternative Studies (ECAS). NASA TM X-71855, 1976.
3. Seikel, G. R.; Staiger, P. J.; and Pian, C. C. P.: Evaluation of the ECAS Open Cycle MHD Power Plant Design. DOE/NASA/2674-78/2, NASA TM-79012, 1978.
4. Svehla, R. A. and McBride, B. J.: FORTRAN IV Computer Program for Calculation of Thermodynamic and Transport Properties of Complex Chemical Systems. NASA TN D-7056, 1973.
5. Smith, J. Marlin and Nichols, L. D.: Estimation of Optimal Operating Conditions for Hydrogen-Oxygen Cesium-Seeded Magnetohydrodynamic Power Generator. NASA TN D-8374, 1977.
6. General Electric/Avco ECAS Task II Oral Briefing, May 9, 1975.
7. Pian, C. C. P.; Seikel, G. R.; Smith, J. Marlin: Performance Calculations for the MHD Generator with Physical Constraints. To be Presented at the 14th Intersociety Energy Conversion Engineering Conference, (Boston, Massachusetts), August 5-10, 1979. Sponsors: ANS, AIChE, SAE, ACS, ASME, IEEE, and AIAA.
8. Doss, E. and Geyer, H.: Two-Dimensional MHD Channel Design and Sectional Optimization with Physical Constraints. Proceedings of 17th Symposium Engineering Aspects of MHD, Stanford, CA, 1978, pp. B.4.1-B.4.8. (CONF-780307-3).
9. Doss, E. et al.: MHD Channel. Technical Support for Open-Cycle MHD Program, ANL/MHD-78-8, Argonne National Laboratory, 1978, pp. 11-21.
10. Ebeling, R. W., Jr.; Burkhart, J. A.; Cutting, J. C.: Oxygen-Enriched Air for MHD Power Plants. To be Presented at the 18th Symposium Engineering Aspects of MHD, (Butte, Montana), June 18-20, 1979. Sponsored by SEAM (Sym. on the Engineering Aspects of MHD).

• • •

TABLE I
MAJOR CYCLE PARAMETERS

Coal type	Illinois #6
Moisture content of coal delivered to combustor, percent	2
Oxidizer preheat temperature, F	1100, 1400, 2000, 2500, 3000
Combustor pressure, atm	Variable
Combustor fuel-oxidizer ratio relative to stoichiometric	1.07
Combustor slag rejection, percent	85, 50, 0
Generator type	Faraday
Potassium seed, seed-coal weight ratio	.108
Diffuser exit pressure, atm	1.14
Diffuser pressure recovery coefficient	0.7, 0.4
Channel length, meters	25, 20
Compressor polytropic efficiency	0.898
Thermal input to generator, MW _{th}	5373
Sulfur removal by seed, percent reduction	81
Inverter efficiency, percent	99
Final fuel-oxidizer ratio relative to stoichiometric	1.0
Stack temperature, F	260
Separately-fired preheater approach temperature difference, F	300
Preheater combustor energy conversion efficiency, percent	100, 90
Steam-turbine generator cycle efficiency, percent	41.8

TABLE I
MAJOR CYCLE PARAMETERS (continued)

Steam turbine-compressor cycle efficiency, 41.3 percent (cycle compressor and air separation plant compressor)

MHD combustor heat loss, percent of thermal input 0.92

Recycle gas to preheater combustor, temperature F 1100

Air preheat to preheater combustor, temperature F 1100

Air separation plant compressor power requirement, kw-hr/ton of equivalent pure oxygen added 300, 200

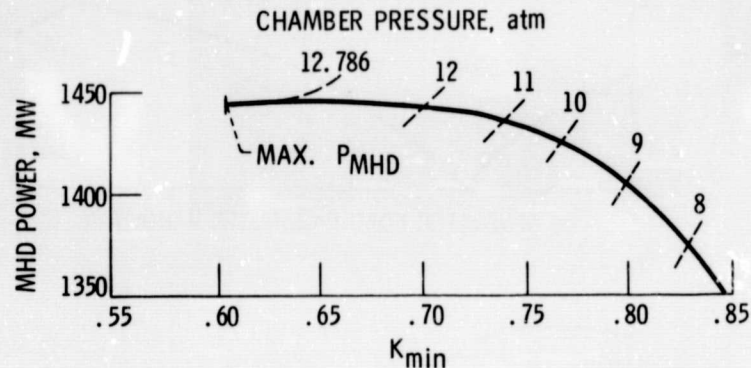
Pressure drop from compressor exit to combustor exit, percent of compressor exit pressure .163

TABLE II

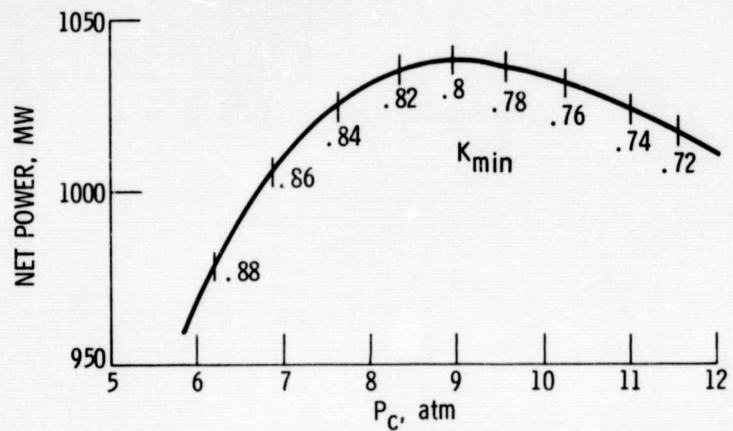
PLANT THERMODYNAMIC EFFICIENCY VARIATION WITH DIFFUSER PERFORMANCE

Direct Preheat Temperature	% Oxygen Enrichment	Plant Thermodynamic Efficiency	
		Diffuser $C_p = 0.4$	$C_p = 0.7$
2500 F	0%	53.49	54.45
1100F	50%	47.75	48.45
	60%	47.92	48.60

Efficiencies are for an oxidant production power requirement of 200 kw-hr/ton of equivalent pure oxygen.



(a) GENERATOR POWER AS A FUNCTION OF MINIMUM LOAD PARAMETER, K_{\min} .



(b) MHD GENERATOR POWER MINUS COMPRESSOR POWER AS A FUNCTION OF COMBUSTOR PRESSURE, P_C .

Figure 1. - Typical MHD generator power variation.
 Oxidizer 2500° F preheated air, generator length 25 m, thermal input 5373 MW, $\gamma_s M^2 = \text{const.}$, $M_{\text{inlet}} = 0.9$, $E_{\text{crit}} = 4000 \text{ V/m}$, $E_{x_{\text{crit}}} = 2500 \text{ V/m}$, $J_{y_{\text{crit}}} = 10000 \text{ A/m}^2$, $\beta_{\text{crit}} = 4$.

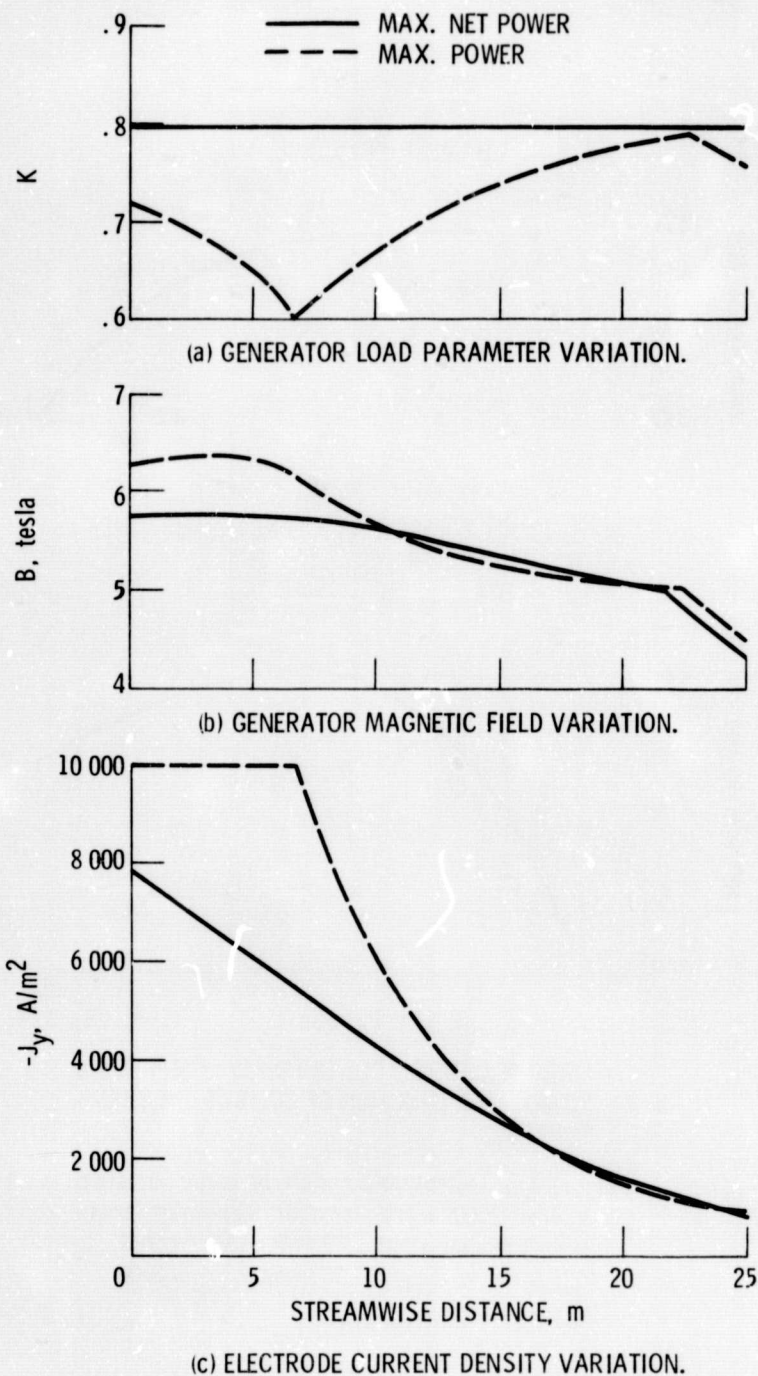


Figure 2. - Parameter distributions for typical MHD generator case. Oxidizer 2500^0 F preheated air, generator length 25 m, thermal input 5373 MW, $\gamma_s M^2 = \text{const.}$, $\lambda_{\text{inlet}} = 0.9$, $E_{\text{crit}} = 4000 \text{ V/m}$, $E_{x_{\text{crit}}} = 2500 \text{ V/m}$, $J_{y_{\text{crit}}} = 10000 \text{ A/m}^2$, $\beta_{\text{crit}} = 4$.

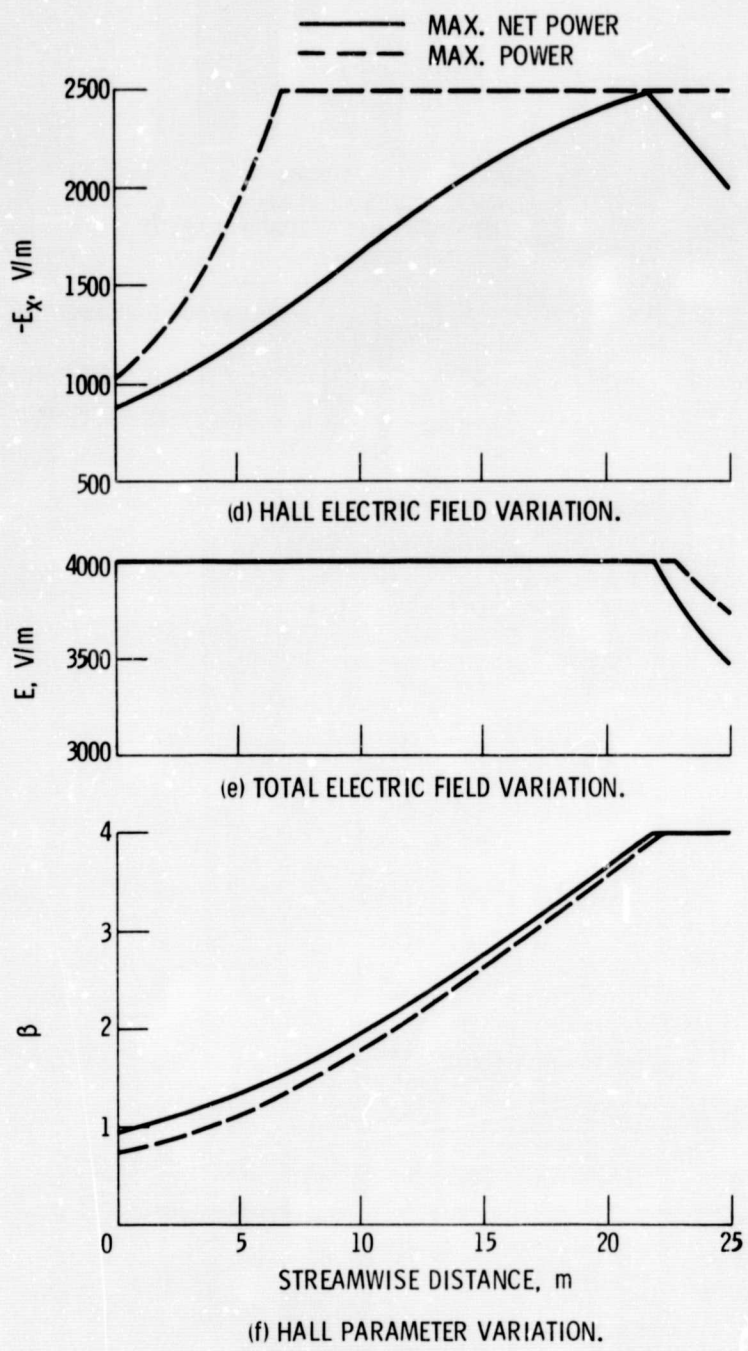


Figure 2. - Concluded.

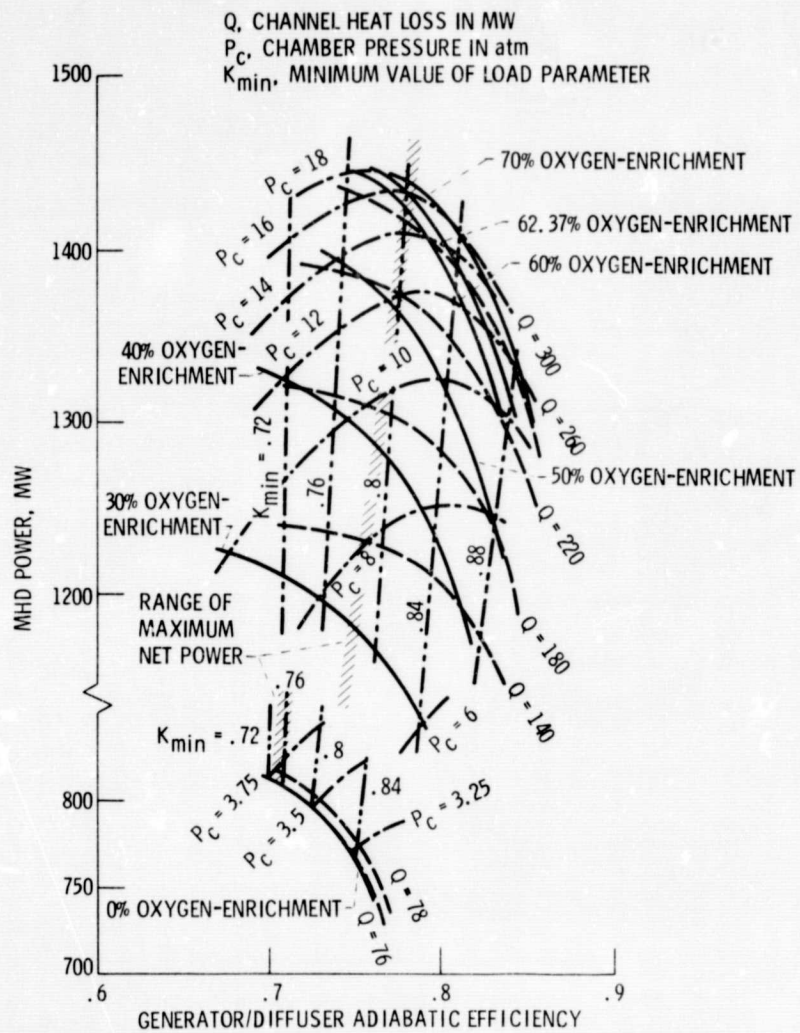


Figure 3. - Generator performance map as a function of oxygen enrichment. Oxygen enriched air for MHD combustor recuperatively preheated to 1100° F. Generator length 25 m, thermal input 5373 MW, $\gamma_s M^2 = \text{const}$, $M_{\text{inlet}} = 0.9$, $E_{\text{crit}} = 4000 \text{ V/m}$, $E_{x_{\text{crit}}} = 2500 \text{ V/m}$, $J_{y_{\text{crit}}} = 10000 \text{ A/m}^2$, $\beta_{\text{crit}} = 4$.

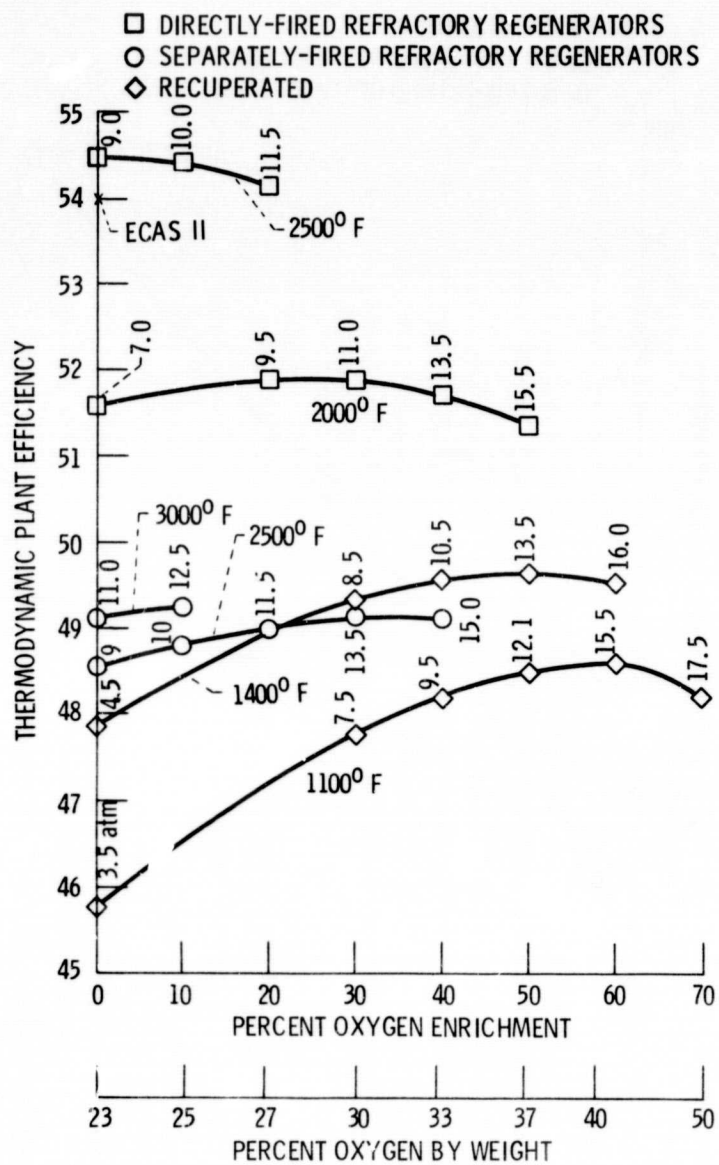


Figure 4. - Plant thermodynamic efficiency as a function of oxygen enrichment for MHD plants with various types of preheater and preheat temperatures. The power required to produce oxygen is 200 kW-hr/ton of equivalent pure oxygen. The combustor pressure in atmospheres is shown along the curves.

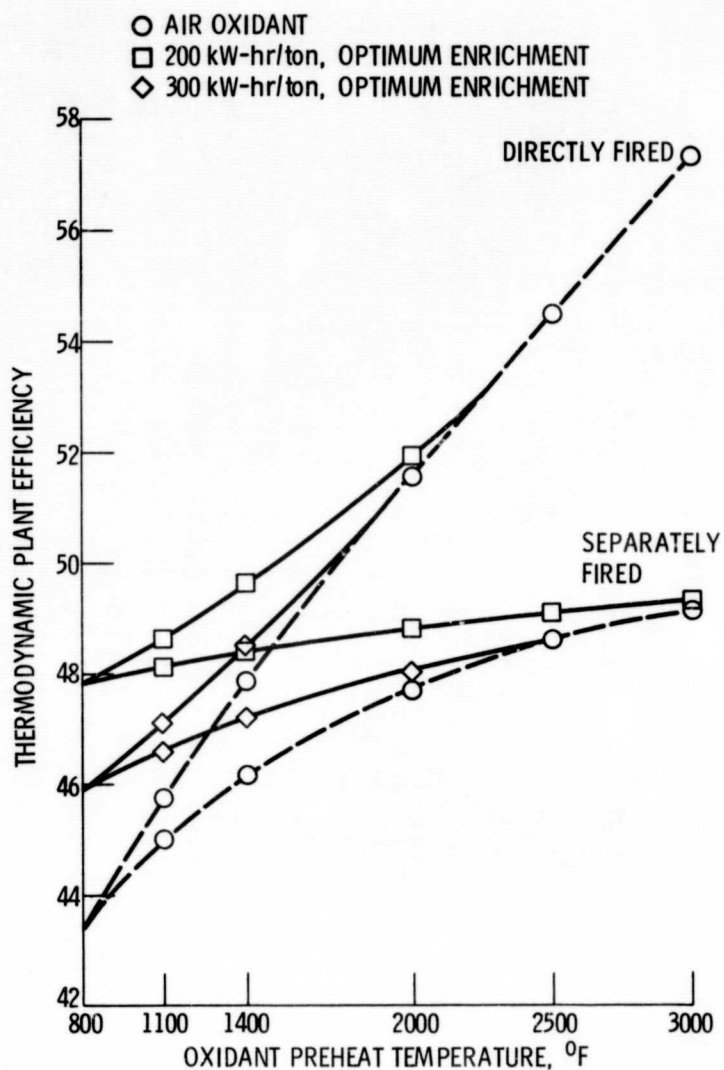
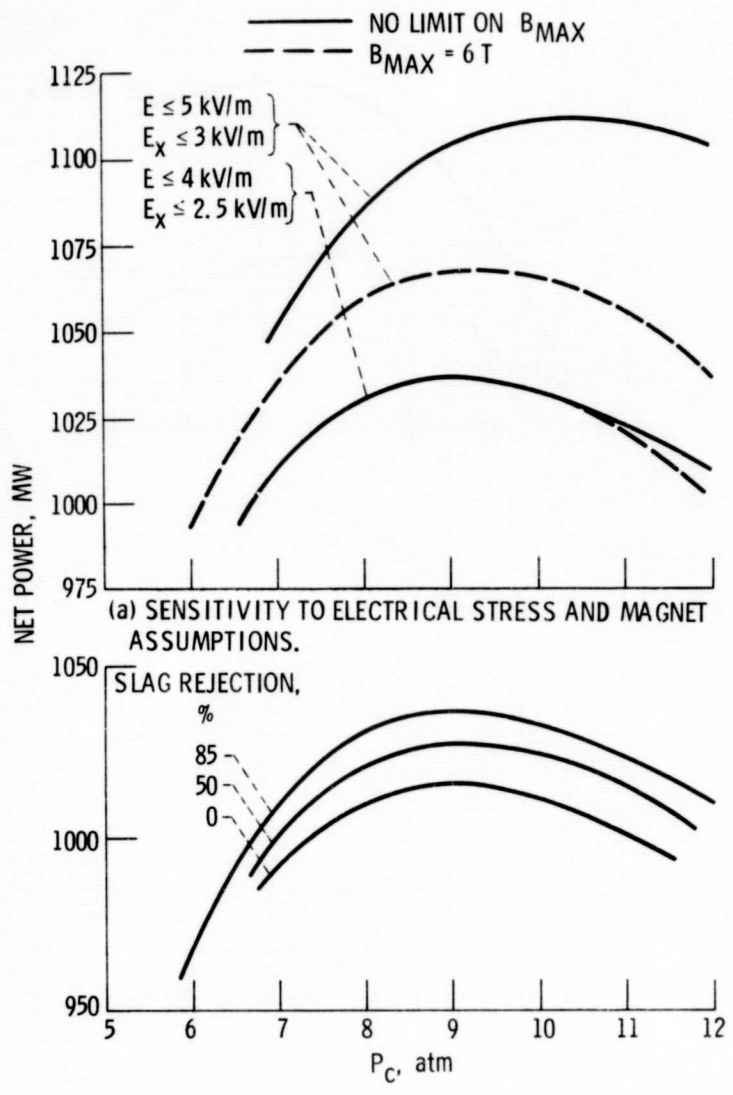
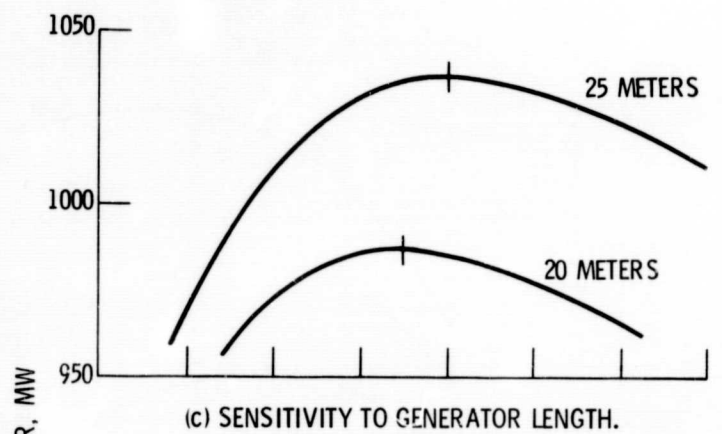


Figure 5. - Comparison of thermodynamic efficiency of MHD plants at optimum oxygen enrichment and for air oxidant. Energy to produce oxygen is on the bases of equivalent pure oxygen. Separately fired preheater system has 90% energy conversion efficiency.

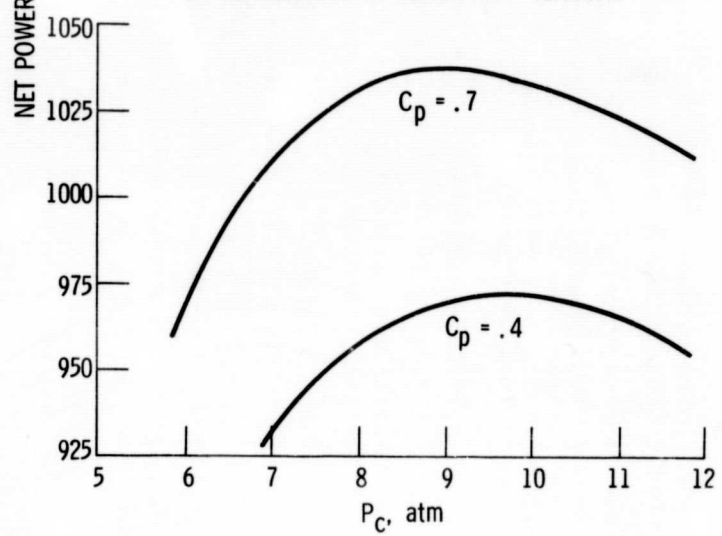


(b) SENSITIVITY TO COMBUSTOR SLAG REJECTION.

Figure 6. - MHD generator minus compressor power variations with assumptions.



(c) SENSITIVITY TO GENERATOR LENGTH.



(d) SENSITIVITY TO DIFFUSER PRESSURE RECOVERY.

Figure 6. - Concluded.

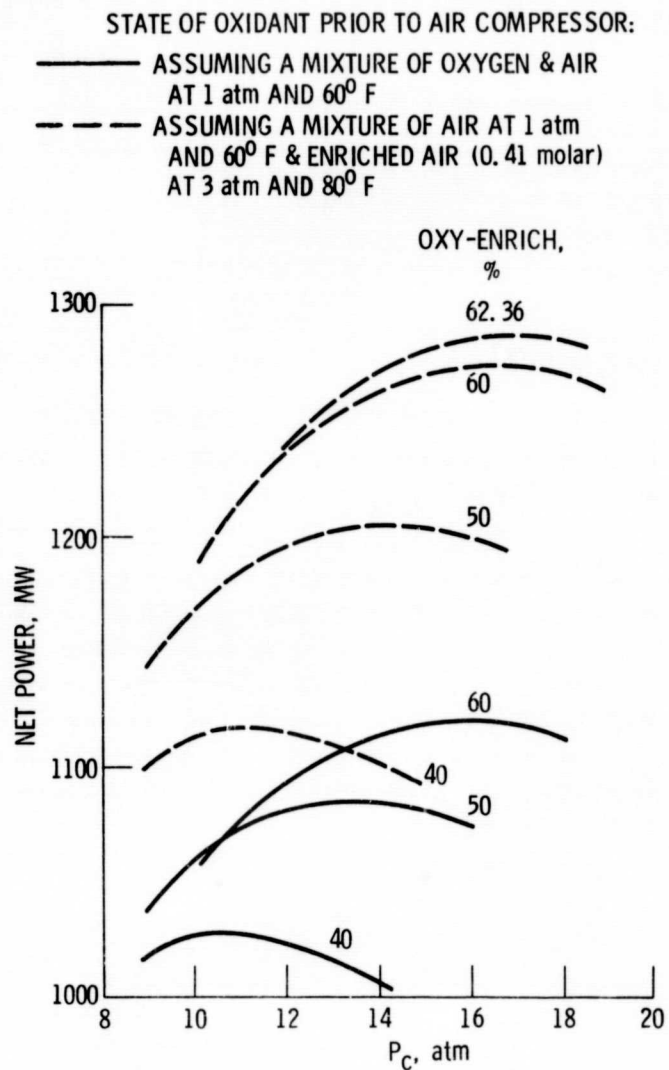


Figure 7. - Net MHD power out as a function of the initial state of the oxidant. Oxidizer 1400° F pre-heated enriched air, generator length 25 m, thermal input 5373 MW, $\gamma_s M^2 = \text{const.}$, $M_{\text{inlet}} = 0.9$, $E_{\text{crit}} = 4000 \text{ V/m}$, $E_{x\text{crit}} = 2500 \text{ V/m}$, $J_{y\text{crit}} = 10\,000 \text{ A/m}^2$, $\beta_{\text{crit}} = 4$.

1. Report No. NASA TM-79140	2. Government Accession No.	3. Recipient's Catalog No.	
4. Title and Subtitle MHD PERFORMANCE CALCULATIONS WITH OXYGEN ENRICHMENT		5. Report Date	
6. Performing Organization Code			
7. Author(s) C. C. P. Pian, P. J. Staiger, and G. R. Seikel		8. Performing Organization Report No. E-9987	
9. Performing Organization Name and Address National Aeronautics and Space Administration Lewis Research Center Cleveland, Ohio 44135		10. Work Unit No.	
11. Contract or Grant No.			
12. Sponsoring Agency Name and Address U. S. Department of Energy Division of Magnetohydrodynamics Washington, D. C. 20545		13. Type of Report and Period Covered Technical Memorandum	
14. Sponsoring Agency Code Report No. DOE/NASA/2674-79/4			
15. Supplementary Notes Prepared under Interagency Agreement EF-77-A-01-2674. Prepared for Eighteenth Symposium on Engineering Aspects of Magnetohydrodynamics, Butte, Montana, June 18-20, 1979.			
16. Abstract The impact of oxygen enrichment of the combustion air on the generator and overall plant performance has been studied for the ECAS-scale MHD/steam plants. A channel optimization technique is described and the results of generator performance calculations using this technique are presented. Performance maps are generated to assess the impact of various generator parameters. Directly and separately preheated plant performance with varying O₂ enrichment is calculated. The optimal level of enrichment is a function of plant type and preheat temperature. The sensitivity of overall plant performance to critical channel assumptions and oxygen plant performance characteristics is also examined.			
17. Key Words (Suggested by Author(s)) Magnetohydrodynamic power generation Oxygen enrichment MHD generator optimization		18. Distribution Statement Unclassified - unlimited STAR Category 44 DOE Category UC-90g	
19. Security Classif. (of this report) Unclassified	20. Security Classif. (of this page) Unclassified	21. No. of Pages	22. Price*